Supplement of Atmos. Chem. Phys., 23, 8259–8269, 2023
https://doi.org/10.5194/acp-23-8259-2023-supplement

Atmospheric Chemistry and Physics
Open Access
EGU

Supplement of

Detection of large-scale cloud microphysical changes within a major shipping corridor after implementation of the International Maritime Organization 2020 fuel sulfur regulations

Michael S. Diamond

Correspondence to: Michael S. Diamond (msdiamond@fsu.edu)

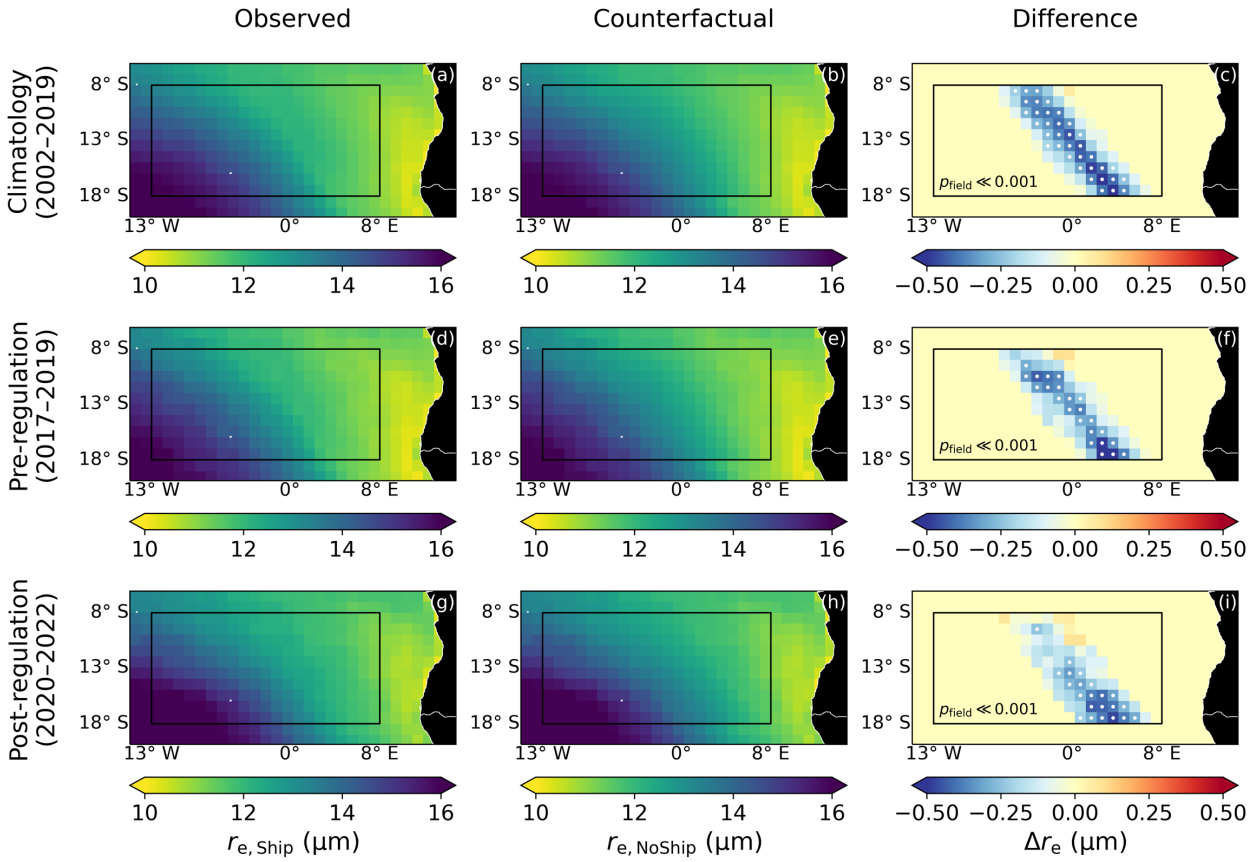

Figure S1. Maps of factual (observed) and counterfactual values and their difference for the annual mean liquid cloud droplet effective radius for the pre-2020 climatology (a–c), the immediately pre-regulation 3-year period 2017–2019 (d–f), and the immediate post-regulation 3-year period 2020–2022 (g–i). The analysis domain of 18° S to 8° S, 13° W to 8° E is outlined in black. Grid points for which the observed values fall outside the 95% confidence interval obtained via kriging are indicated by white dots and the corresponding field significance values are reported in (c,f,i).

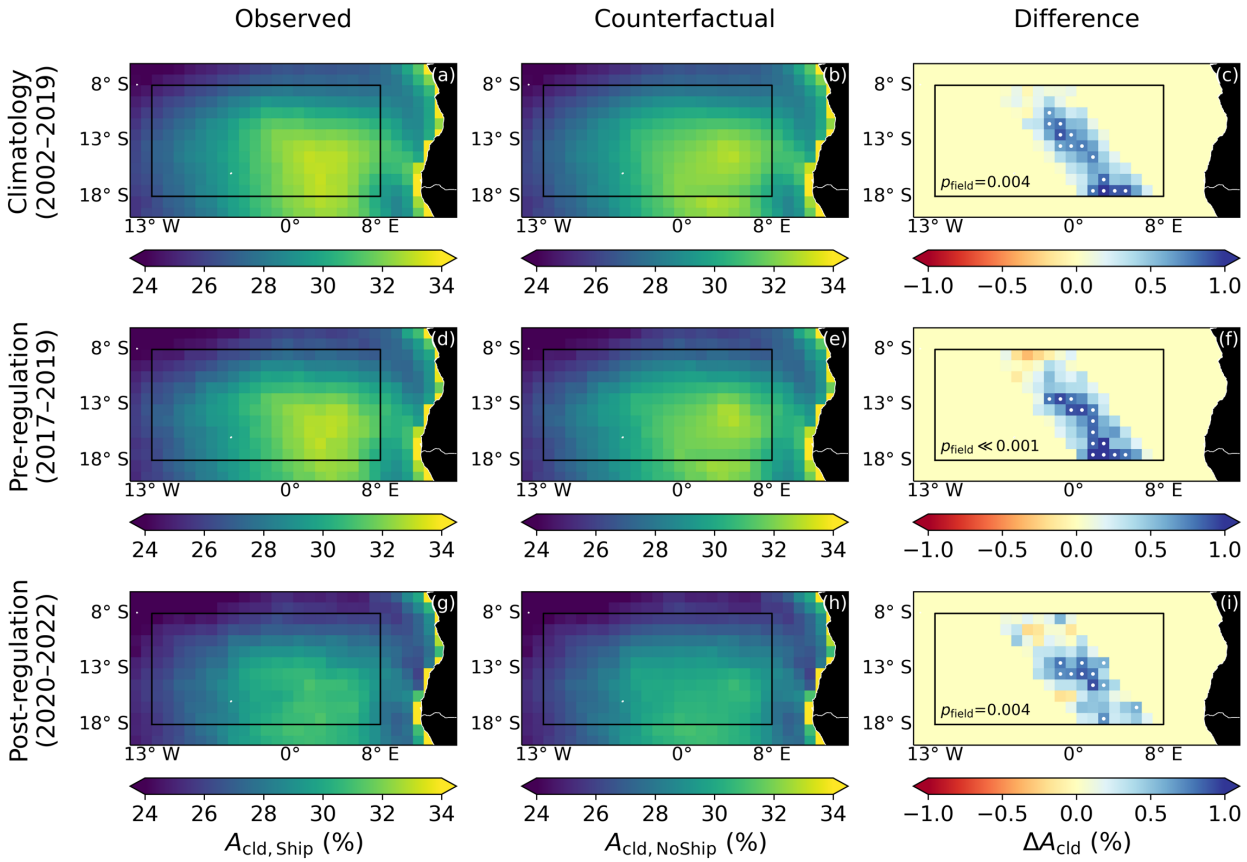

Figure S2. As in Figure S1, but for the annual mean overcast albedo.

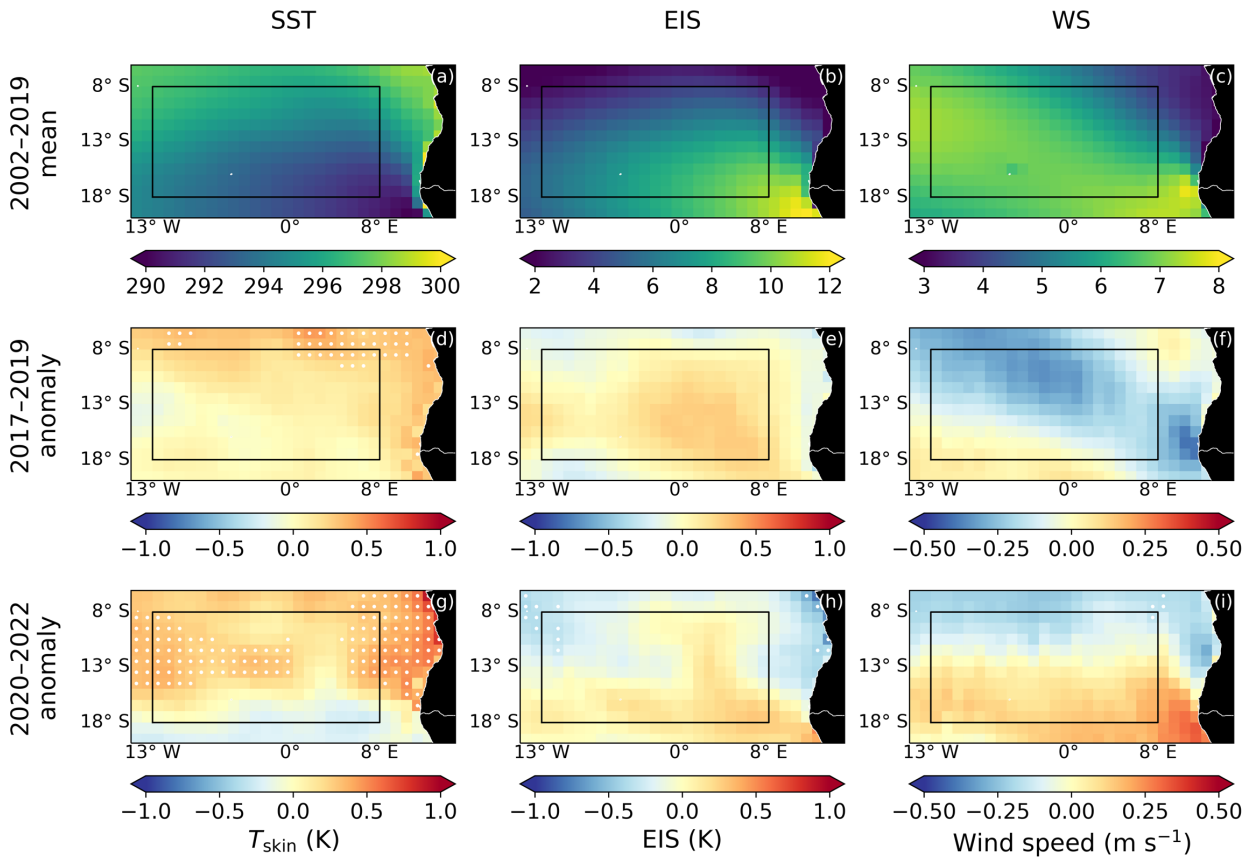

Figure S3. Maps of austral spring surface skin temperature (SST), estimated inversion strength (EIS), and wind speed (WS) mean values for the pre-2020 climatology (a–c) and anomalies from the 2002-2019 mean for 2017-2019 (d–f) and 2020-2022 (g–i). The analysis domain of 18° S to 8° S, 13° W to 8° E is outlined in black. Grid points for which the anomaly magnitudes exceed two standard deviations of the set of 2002–2004, 2005–2007, 2008–2010, 2011–2013, 2014–2016, and 2017–2019 mean values are indicated by white dots in (d–i).

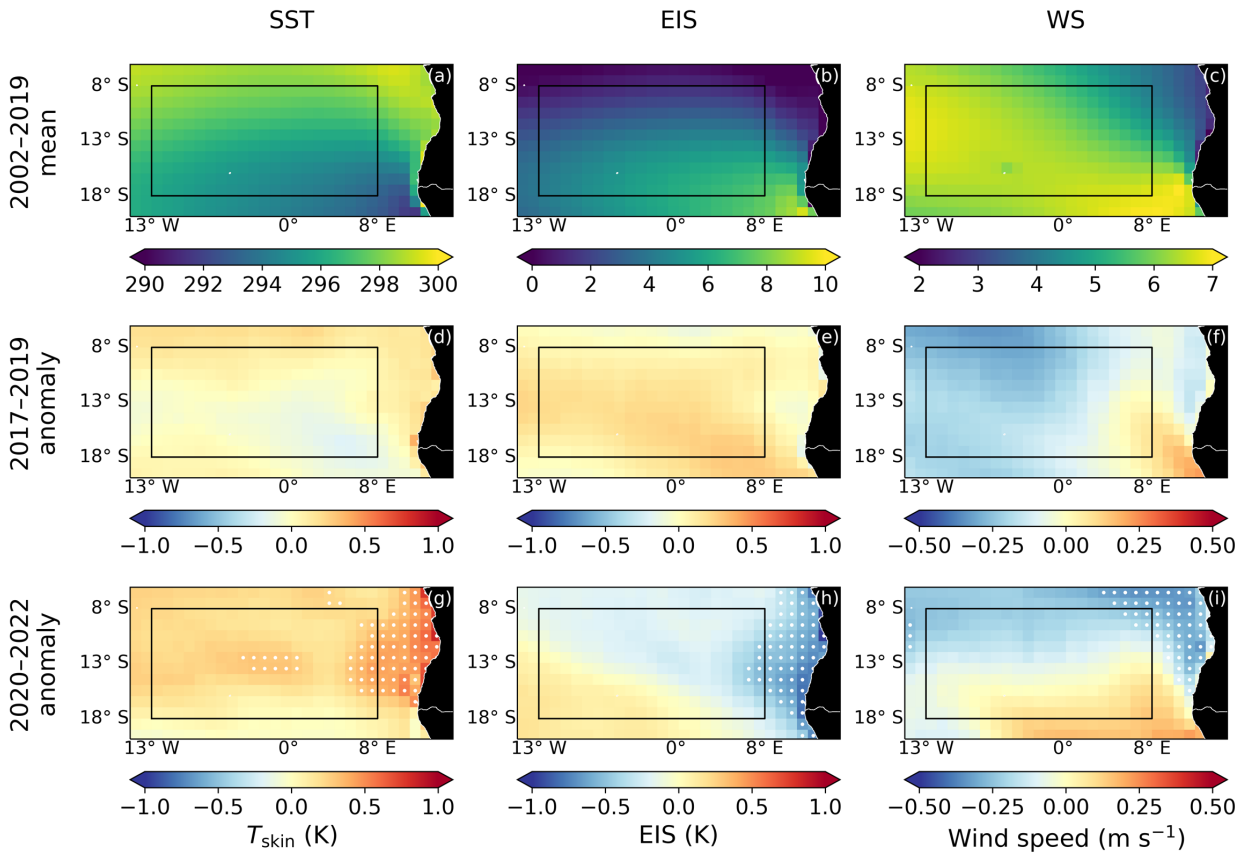

Figure S4. As in Figure S3, but for the annual mean surface skin temperature, estimated inversion strength, and wind speed.

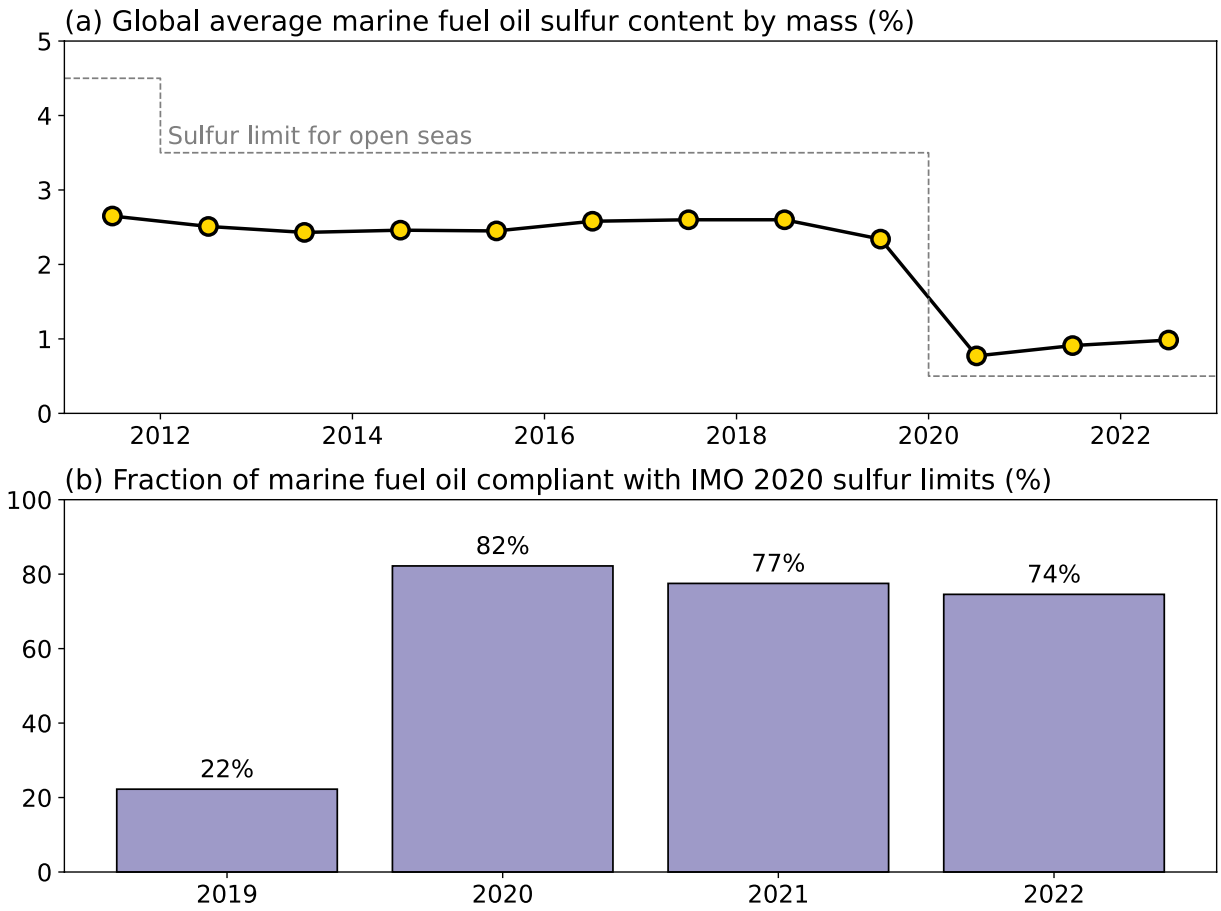

Figure S5. Marine fuel oil statistics (combined residual and distillate) — compiled by Lloyd's Register EMEA, Veritas Petroleum Services B.V., and Viswa Lab and reported to the IMO MEPC — shown as annual global averages of sulfur mass content for marine fuel oils (a) and the percentage of marine fuel oils, by mass, below 0.5% sulfur mass content (b). The sulfur limit for open seas is shown as a gray dotted line in (a) for reference.

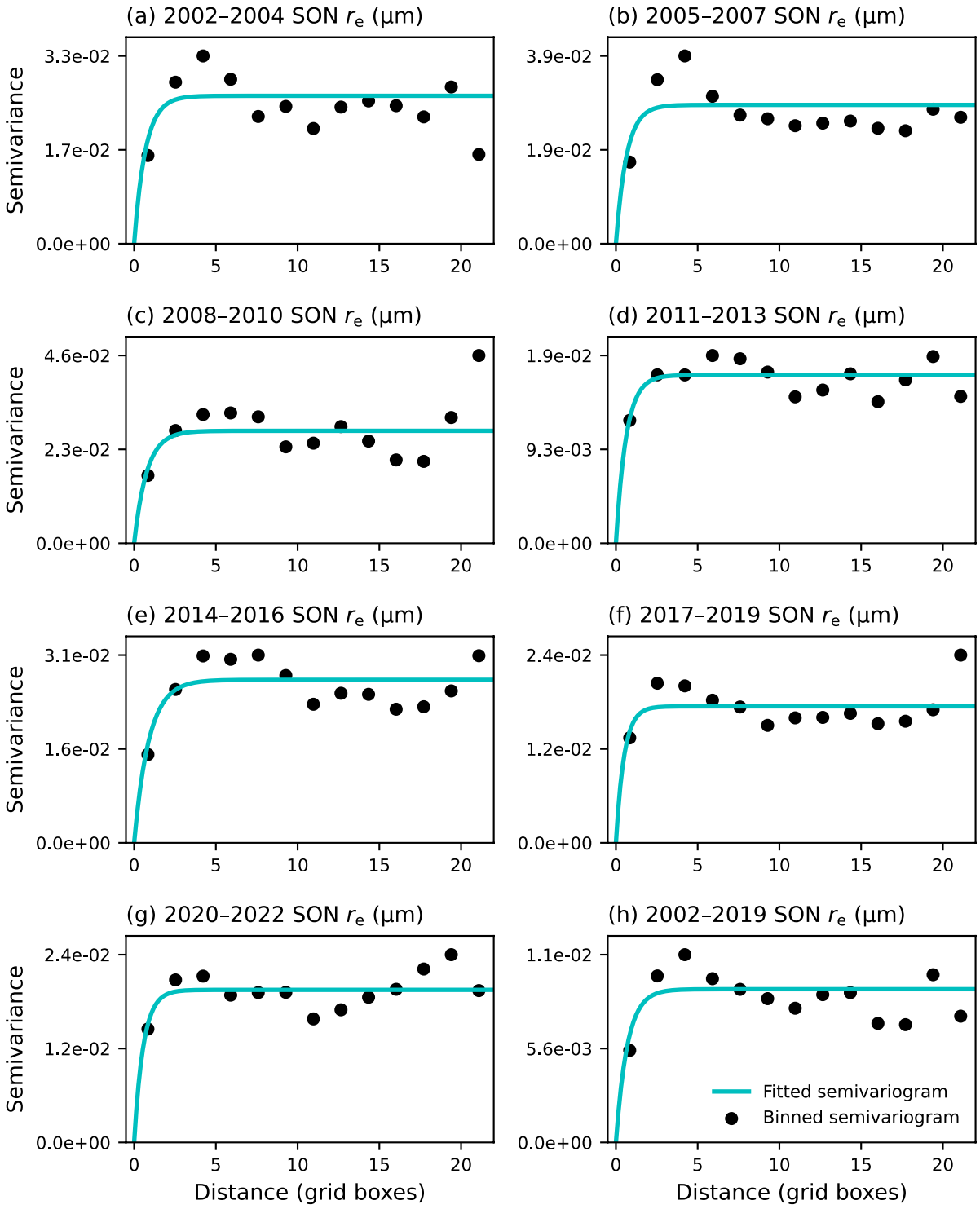

Figure S6. Semivariograms for austral spring liquid cloud effective radius.

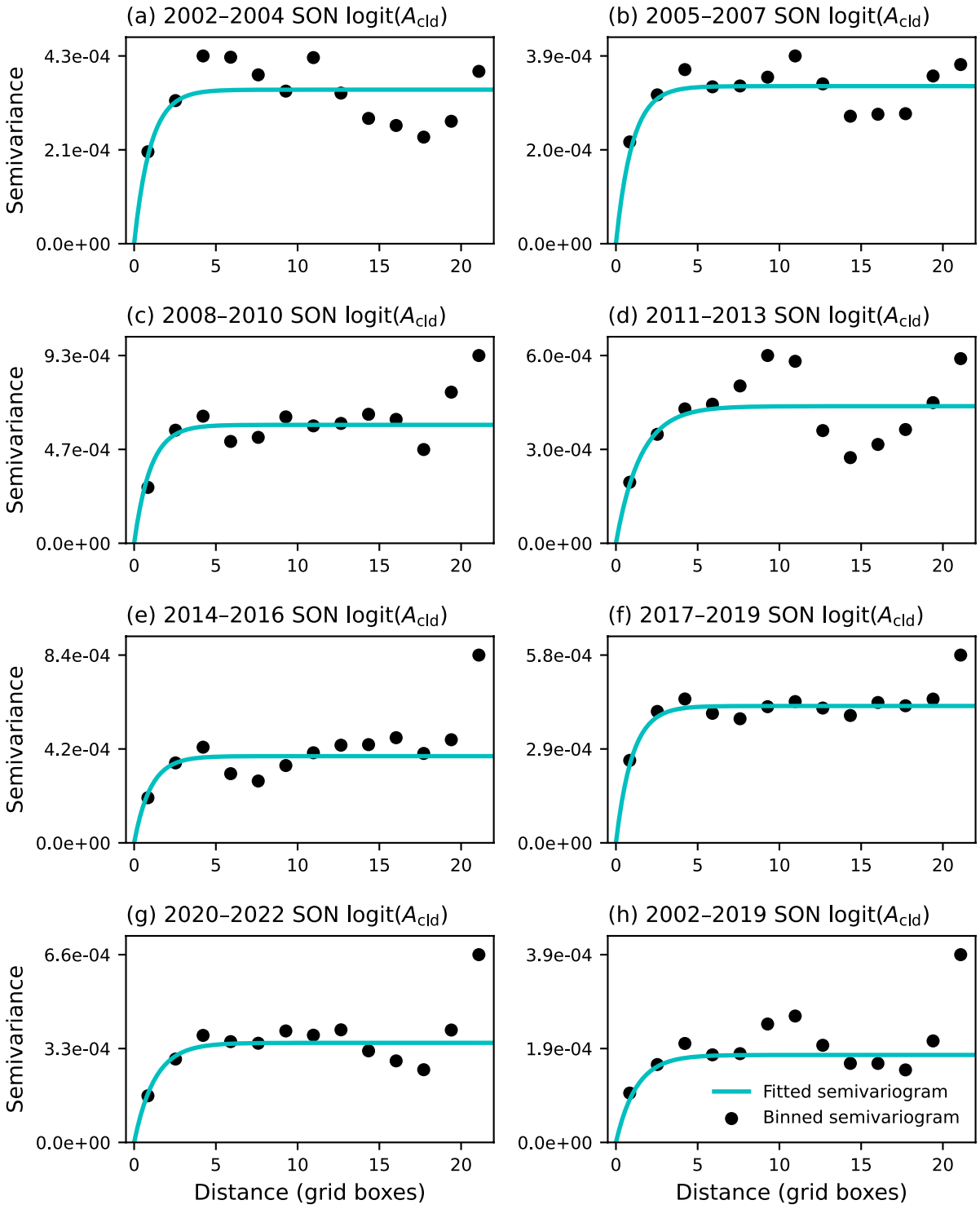

Figure S7. Semivariograms for austral spring overcast albedo.

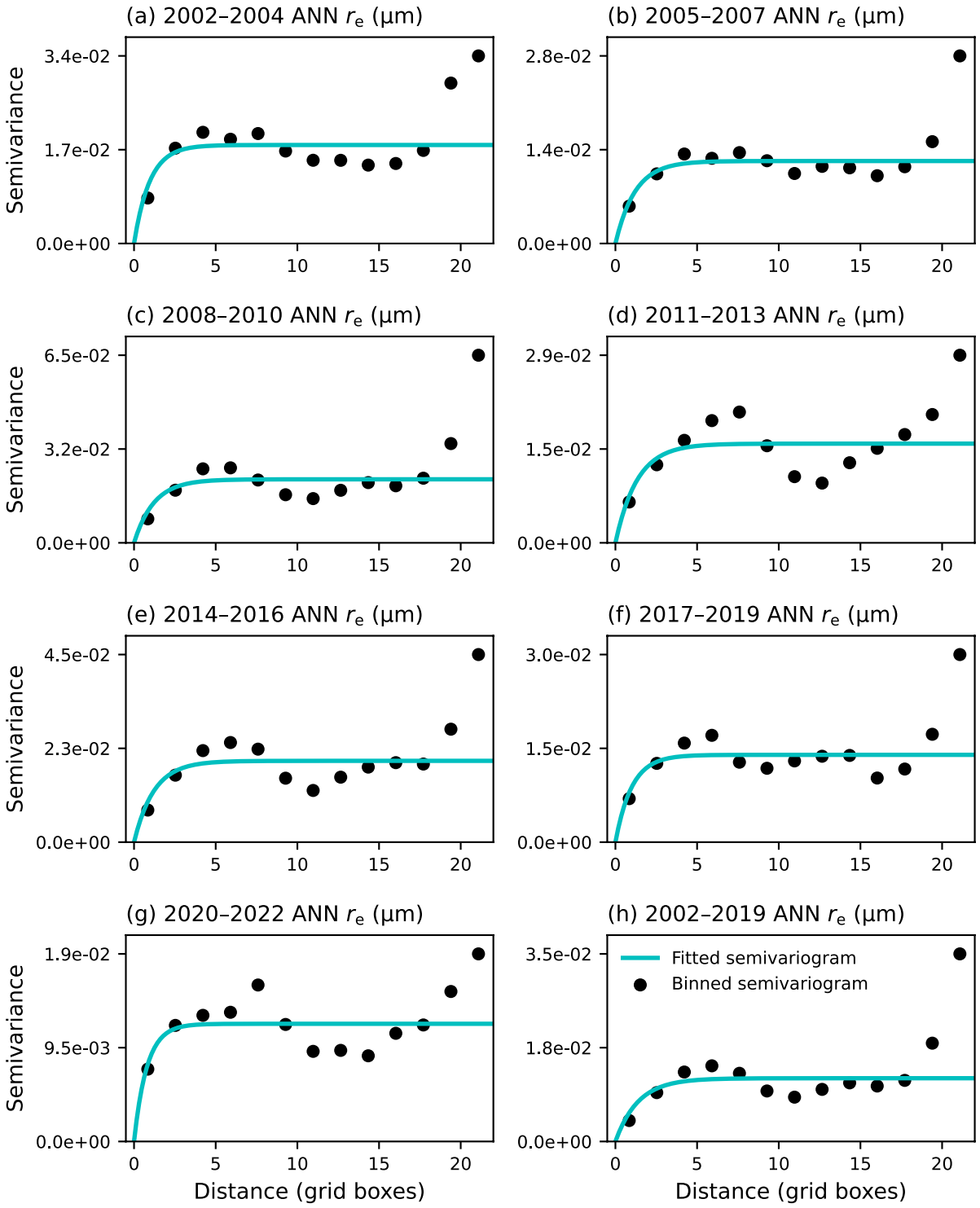

Figure S8. Semivariograms for annual mean liquid cloud effective radius.

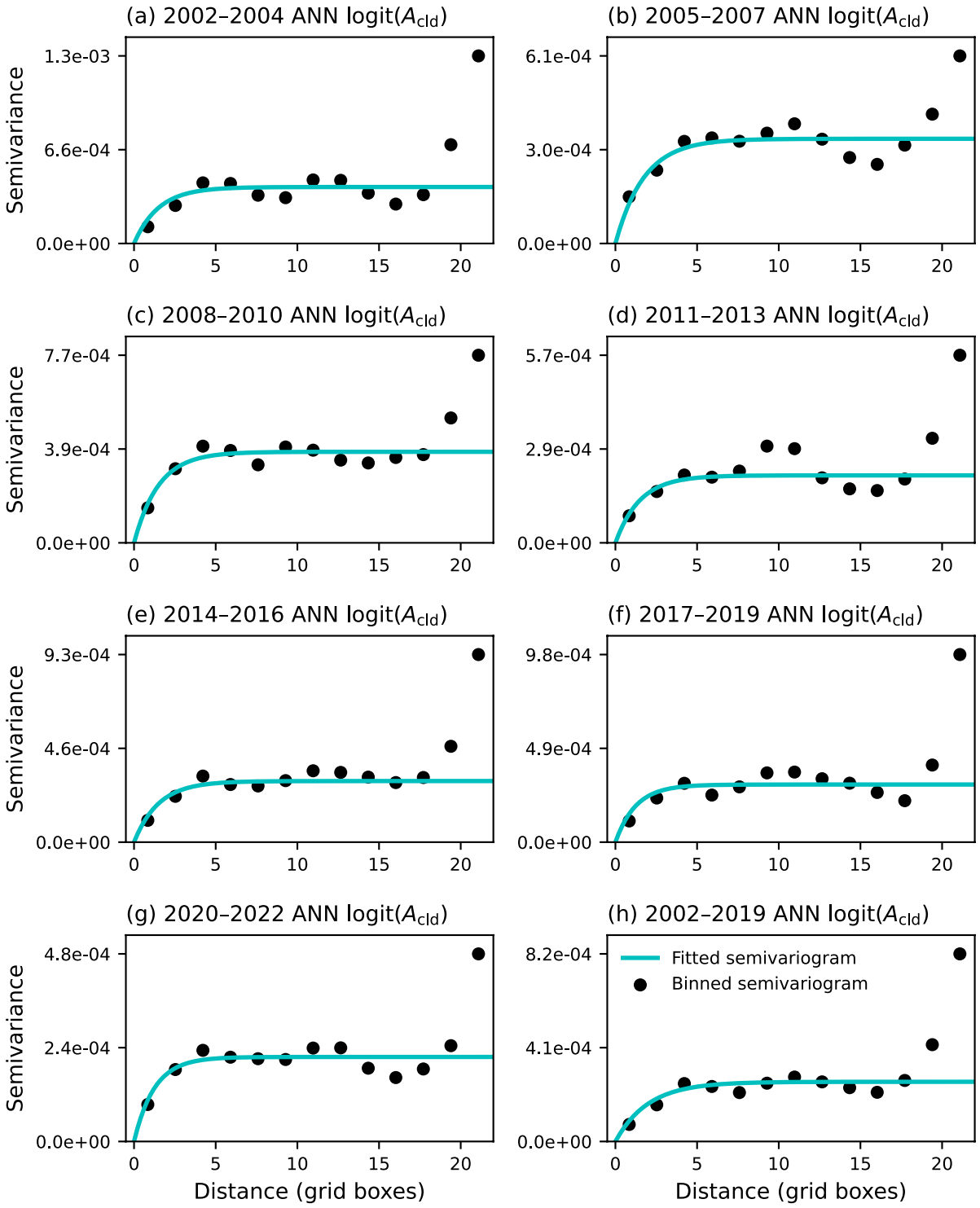

Figure S9. Semivariograms for annual mean overcast albedo.

Table S1. Summary of statistics (mean Ship value, absolute and relative Ship-NoShip difference, and field significance) and regressors used for the mean function in the kriging implementation (as selected via minimization of the Bayesian information criterion) for austral spring and annual mean values of the liquid cloud droplet effective radius and overcast albedo fields.

Years	Mean Ship	Absolute Ship-NoShip difference	Relative Ship-NoShip difference (%)	Field significance	Regressors used
Austral spring liquid cloud droplet effective radius (μm)					
2002–2004	12.02	-0.37 (-0.48 to -0.26)	-3.0 (-4.0 to -2.1)	< 0.0001	lon, lon^2, lat^2, lon*lat
2005–2007	12.54	-0.56 (-0.67 to -0.45)	-4.4 (-5.3 to -3.5)	< 0.0001	WS, lon, lon^2, lat, lat^2, lon*lat
2008–2010	12.47	-0.76 (-0.88 to -0.65)	-6.1 (-7.1 to -5.2)	< 0.0001	lon, lon^2, lat, lat^2, lon*lat
2011–2013	12.57	-0.62 (-0.70 to -0.54)	-4.9 (-5.6 to -4.3)	< 0.0001	EIS, WS, lon^2, lat, lat^2, lon*lat
2014–2016	12.37	-0.49 (-0.62 to -0.37)	-4.0 (-5.0 to -3.0)	< 0.0001	EIS, WS, lon, lon^2, lat, lat^2, lon*lat
2017–2019	12.44	-0.46 (-0.54 to -0.38)	-3.7 (-4.3 to -3.1)	< 0.0001	EIS, WS, lon^2, lat, lat^2, lon*lat
2020–2022	13.14	-0.16 (-0.25 to -0.08)	-1.3 (-1.9 to -0.6)	0.00197	SST, lon, lon^2, lat, lat^2, lon*lat
2002–2019	12.40	-0.56 (-0.63 to -0.50)	-4.5 (-5.1 to -4.0)	< 0.0001	SST, WS, lon, lon^2, lat, lat^2, lon*lat
Austral spring overcast albedo (%)					
2002–2004	35.71	0.61 (0.26 to 0.95)	1.7 (0.7 to 2.7)	0.00056	SST, EIS, WS, lon^2, lat, lat^2
2005–2007	36.78	1.10 (0.75 to 1.43)	3.0 (2.0 to 3.9)	< 0.0001	SST, EIS, WS, lon, lon^2, lat^2, lon*lat
2008–2010	36.13	1.12 (0.68 to 1.55)	3.1 (1.9 to 4.3)	< 0.0001	SST, EIS, lon, lon^2, lat^2
2011–2013	37.00	0.85 (0.42 to 1.28)	2.3 (1.1 to 3.5)	< 0.0001	SST, EIS, WS, lon^2, lon*lat
2014–2016	36.24	0.61 (0.23 to 0.98)	1.7 (0.6 to 2.7)	0.00356	SST, WS, lon, lon^2, lat, lat^2, lon*lat
2017–2019	35.12	0.83 (0.44 to 1.22)	2.4 (1.3 to 3.5)	< 0.0001	SST, EIS, WS, lon, lon^2, lat, lat^2, lon*lat
2020–2022	34.79	0.36 (-0.004 to 0.71)	1.0 (-0.01 to 2.1)	0.00375	WS, lon^2, lat, lat^2, lon*lat
2002–2019	36.16	0.78 (0.52 to 1.04)	2.1 (1.4 to 2.9)	< 0.0001	SST, EIS, WS, lon, lon^2, lat, lon*lat
Annual mean liquid cloud droplet effective radius (μm)					
2002–2004	12.02	-0.40 (-0.50 to -0.29)	-3.3 (-4.2 to -2.4)	< 0.0001	WS, lon^2, lat^2, lon*lat
2005–2007	12.25	-0.42 (-0.51 to -0.32)	-3.4 (-4.2 to -2.6)	< 0.0001	SST, lon^2, lat, lat^2, lon*lat
2008–2010	12.32	-0.37 (-0.50 to -0.25)	-3.0 (-4.0 to -2.0)	< 0.0001	SST, EIS, WS, lon, lon^2, lon*lat
2011–2013	12.21	-0.39 (-0.50 to -0.28)	-3.2 (-4.1 to -2.3)	< 0.0001	EIS, WS, lon, lon^2, lat, lon*lat
2014–2016	12.33	-0.38 (-0.50 to -0.26)	-3.1 (-4.1 to -2.1)	< 0.0001	WS, lon, lon^2, lat, lat^2, lon*lat
2017–2019	12.08	-0.31 (-0.39 to -0.22)	-2.5 (-3.2 to -1.8)	< 0.0001	SST, EIS, WS, lon, lat^2, lon*lat
2020–2022	12.51	-0.24 (-0.32 to -0.17)	-1.9 (-2.6 to -1.3)	< 0.0001	EIS, WS, lon, lat, lat^2, lon*lat
2002–2019	12.20	-0.37 (-0.47 to -0.28)	-3.1 (-3.8 to -2.3)	< 0.0001	EIS, WS, lon, lon^2, lat, lon*lat
Annual mean overcast albedo (%)					
2002–2004	31.72	0.60 (0.23 to 0.96)	1.9 (0.7 to 3.0)	0.05960	EIS, lon, lon^2, lat, lat^2, lon*lat
2005–2007	31.89	0.67 (0.33 to 1.01)	2.1 (1.0 to 3.2)	0.00179	SST, EIS, WS, lon, lon^2
2008–2010	30.79	0.59 (0.23 to 0.96)	1.9 (0.8 to 3.1)	0.02622	SST, EIS, WS, lon, lon^2, lon*lat
2011–2013	31.68	0.52 (0.25 to 0.79)	1.6 (0.8 to 2.5)	< 0.0001	SST, lon, lon^2, lat, lat^2, lon*lat
2014–2016	31.43	0.68 (0.36 to 1.00)	2.2 (1.1 to 3.2)	0.00029	SST, lon, lon^2, lat, lat^2, lon*lat
2017–2019	30.98	0.54 (0.23 to 0.85)	1.8 (0.7 to 2.7)	0.0008	lon, lon^2, lat, lat^2, lon*lat
2020–2022	29.33	0.38 (0.12 to 0.62)	1.3 (0.4 to 2.1)	0.00427	SST, EIS, WS, lon, lon^2, lat, lat^2, lon*lat
2002–2019	31.41	0.56 (0.26 to 0.85)	1.8 (0.8 to 2.7)	0.00366	SST, EIS, lon^2, lat, lat^2, lon*lat

Table S2. Percentiles of the estimated reduction in shipping effects after the implementation of the marine fuel sulfur regulations in 2020, as measured by the ratio of the 2020-2022 relative Ship-NoShip difference to the climatological 2002–2019 value for the austral spring (SON) and annual mean (ANN) liquid cloud droplet effective radius (r_e) and overcast albedo (A_{cld}) fields. Values are emboldened to indicate whether the ratios show statistically significant decreases at different thresholds (50th for median value only, 25th-75th for interquartile range, 5th–95th for 90% confidence, 2.5th–97.5th for 95% confidence, and 0.5th–99.5th for 99% confidence interval).

Variable	Percentile of 2020–2022 relative difference over 2002–2019 value ratio								
	0.5th	2.5th	5th	25th	50th	75th	95th	97.5th	99.5th
SON r_e	**0.09**	**0.13**	**0.15**	**0.23**	**0.27**	**0.33**	**0.41**	**0.43**	**0.48**
SON A_{cld}	-0.18	-0.01	**0.08**	**0.31**	**0.48**	**0.66**	**0.97**	1.08	1.38
ANN r_e	0.36	**0.41**	**0.44**	**0.55**	**0.64**	**0.73**	**0.89**	**0.95**	1.07
ANN A_{cld}	0.06	0.22	0.29	**0.53**	**0.72**	**0.96**	1.50	1.76	2.57